Biotin-Initiated Poly(Oxazoline)s

Joseph A. Garcia, Ashley Vergara Mendez, Ellen M. Sletten*

J. A. Garcia, A. Vergara Mendez, E. M. Sletten. Department of Chemistry and Biochemistry, University of California, Los Angeles 607 Charles E. Young Dr. East, Los Angeles, CA 90095 (USA)
*E-mail: Sletten@chem.ucla.edu

KEYWORDS: poly(oxazoline), biotin, initiation

ABSTRACT: Biotinylated hydrophilic polymers are used in a plethora of chemical and biochemical assays due to the exceptional affinity of biotin for (strept)avidin. Here we report a facile method for the installation of biotin at the end of poly(oxazoline)s (P(Ox)) using an electrophilic biotin initiator. While this method is applicable to many different oxazoline monomers, we focus on biotin-poly(2-methyl-2-oxazoline) as it is a desirable alternative to poly(ethylene glycol) (PEG), which has rising immunogenicity concerns. A further advantage of POx over PEG is the high degree of chemical flexibility that can be imparted, which we showcase through the preparation of varied molecular weight, amphiphilic, and bifunctional POxs. Furthermore, we demonstrate the high efficacy of these biotin polymers through a series of common biochemical assays that frequently utilize the biotin-streptavidin pair.

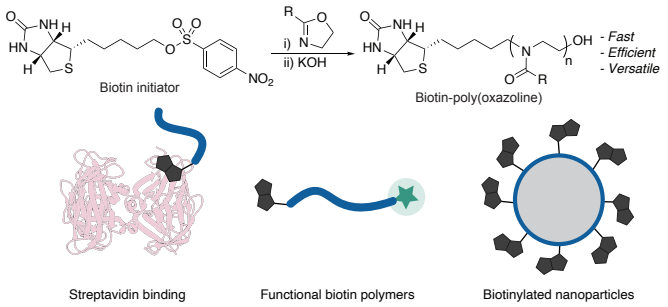

Introduction.

Biotin bearing polymers have pervaded the fields of both chemistry and biology due to the high binding affinity (K_d = 1.3x10^{-15} M) and broad utility of the streptavidin and biotin interaction.[1,2] Applications that utilize biotinylated polymers include immunoprecipitation assays,[3–5] surface functionalization,[6–8] targeted drug delivery,[9–14] fluorescent analyte detection,[15–17] and the study of substrate-enzyme pairs[18–20] (**Figure 1A**). The utilization of polymer or oligomer linkers between biotin and a ligand of interest allows for sufficient spacing for the necessary binding interactions to occur.[21,22] Poly(ethylene glycol) (PEG) is the most commonly used biotinylated polymer scaffold, as PEG itself comes with the distinct advantages of increasing serum half-lives of proteins, reducing interactions with endogenous biomolecules, and enhancing water solubility.[23] However, its frequent use in pharmacological formulations has led to the generation of α-PEG antibodies and enzymes capable of PEG metabolism, leading to immunogenicity and degradation concerns with this polymer scaffold.[24,25] Furthermore, commercially available biotin-PEGs are expensive and come in only a limited selection of molecular weights. While methods have been reported to install biotin directly onto other polymer scaffolds,[8,26–30] efforts to facilely synthesize biotinylated polymers specifically as PEG replacements have yet to be reported.

Poly(oxazoline) (P(Ox)) has entered the field as a desirable alternative to PEG. Poly(2-methyl-2-oxazoline) (P(MeOx)), specifically, retains the aforementioned benefits of PEG and displays superior hydrophilicity, comparable antifouling properties, and a high degree of molecular weight and functional group tunability.[31,32] Due to its limited clinical and cosmetic use, P(MeOx) does not yet have the immunogenic concerns reported in PEG formulations, making it a viable alternative for both *in vitro* and *in vivo* applications. Accordingly, a POx-drug conjugate is currently undergoing phase 1 clinical trials for the treatment of Parkinson's disease.[33]

Single biotin molecules have been previously added onto P(Ox) scaffolds through post-polymerization click chemistry at the initiator or side chain positions, or through post-polymerization carbodiimide chemistry at the terminal end (**Figure 1B**).[33–35] These approaches are disadvantageous because they introduce biotin at subquantitative yields (73 %), are slow (48 h), require an additional step, and/or lack stoichiometric control. Installing biotin in a controlled and efficient manner would increase the utility and accessibility of biotinylated-P(Ox)s. A more reliable and efficient approach would be to introduce biotin as either an electrophilic initiator or a nucleophilic terminator. While the termination of P(Ox) using carboxylic acids is precedented in the literature,[36] the resulting ester functionality can be biologically labile. Furthermore, (D)+biotin (**1**) contains several potentially interfering

functional groups that could hinder efficient end capping. Thus, we sought to turn biotin into an efficient electrophilic initiator for ring-opening polymerization of oxazolines.

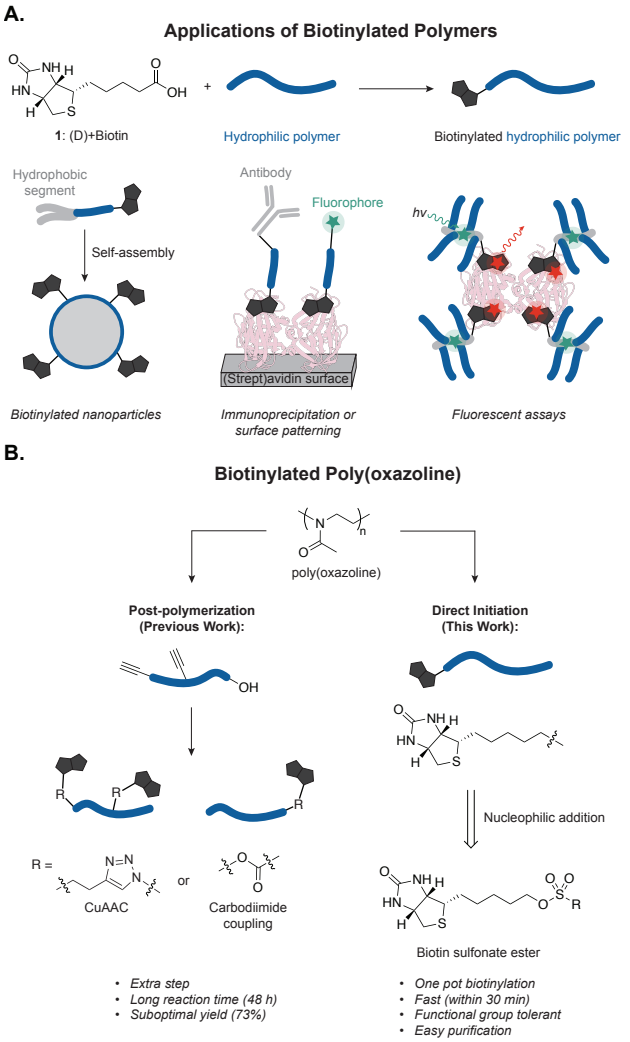

Figure 1. Biotinylation of hydrophilic polymers. A) Applications of biotin polymers. B) Previous work on biotinylated P(Ox) relies solely on post polymerization modifications. Work described herein: rapid and direct biotinylation of P(Ox) using an electrophilic initiator.

To synthesize a biotin initiator, we considered modifying the carboxylic acid. This functional group protrudes out of the binding pocket of streptavidin and is the standard point of conjugation via amide bond formation.[2,37] Fortunately, modifications to this position cause inconsequential changes to the overall binding affinity to streptavidin[1] While acid halide initiators have been reported for the living cationic ring opening polymerization of P(MeOx), halide counterions tend to yield slow rates of polymerization and can sometimes lead to poor initiation.[38,39] Alkyl sulfonate esters, on the other hand, have proven to be excellent initiators for P(MeOx).[36,40,41] These polymerizations initiate fast, the byproducts do not interfere with the propagation, and the resulting polymers bear dispersities ($Đ$) of < 1.2 (indicating a controlled mechanism). Several different alkyl sulfonate esters can be formed readily from a common alcohol precursor. Thus, we prepared a panel of alkyl sulfonate esters from biotinol and evaluated their ability to initiate poly(oxazoline) synthesis. Ultimately, we report the first electrophilic biotin initiator for the ring opening polymerization of P(Ox) and establish an efficient route to synthesize highly functional biotinylated polymers.

Results and Discussion.

Synthesis of biotin initiators.

(D)+biotin (**1**) was esterified and reduced to biotinol (**2**) following established procedures.[42] From this common intermediate, a panel of alkyl sulfonate derivates was synthesized (**3-5, Scheme 1**). Mesylate **3** and tosylate **4** were prepared utilizing mesyl anhydride and tosyl anhydride respectively.[43] 4-nitrobenzene sulfonic anhydride (Ns_2O) was not commercially available, so 4-nitrobenzene sulfonyl chloride (NsCl) was used. This synthesis required Ag_2CO_3 to sequester free chloride anions, which prevented the formation of a chlorinated biotin[43] and allowed for the isolation of biotin nosylate **5**. Significant attempts were made to synthesize the trifluoromethylsulfonate analogue. However, this product would readily dimerize, impeding isolation. Nevertheless, we moved forward with the panel of three initiators for oxazoline polymerization.

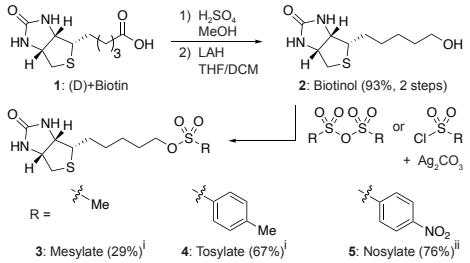

Scheme 1. Synthesis of a panel of electrophilic biotin initiators. Mesylate **3**, tosylate **4**, and nosylate **5** were all accessed from a common biotinol precursor. i) Sulfonate anhydride, pyridine, DCM, rt. ii) 4-nitrobenzene sulfonyl chloride, pyridine, Ag_2CO_3, DCM, rt.

Initiator Evaluation.

Initial polymerizations were conducted to evaluate initiators **3-5** (**Figure 2A**). *N,N*-dimethylacetamide (DMAc) was chosen as the reaction solvent due to its ability to readily solvate all of the initiators and established compatibility with POx polymerizations.[44] While any oxazoline monomer could be utilized, 2-methyl-2-oxazoline (MeOx) was chosen as the monomer to create hydrophilic PEG alternatives.[31] A monomer concentration of 1.25 M with conventional heating at 100 °C was used to compare these initiators directly with reported initiators for P(MeOx). Gratifyingly, all initiators produced polymers with biotin ^{1}H nuclear magnetic resonance (NMR) peaks after dialysis. All initiators yielded polymers with narrow dispersities ($Đ$ < 1.2), but only the tosylate **4** and nosylate **5** initiated polymers reached molecular weights close to the target (3630 Da) as measured by size exclusion chromatography (SEC) (**Figure 2B,** entries 2 and 3). Notably, the tosylate **4** initiated polymer gave a much larger discrepancy in molecular weight between NMR and SEC compared to

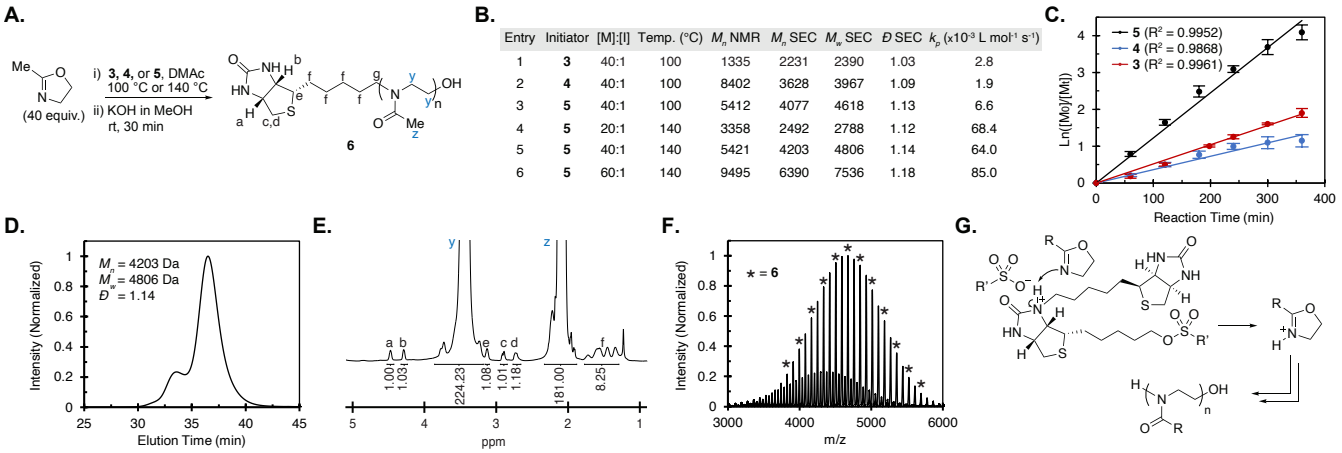

Figure 2. Biotin-P(MeOx) characterization. A) Synthesis of biotin-P(MeOx) using initiators **3**-**5**. B) Polymerization characterization of biotin-P(MeOx) using initiators **3**-**5** at 100 °C, or initiator **5** at 140 °C with varying feed ratios. C) Semi-logarithmic kinetics plots of polymerizations initiated by **3**-**5**. D) Representative SEC trace of **6** at n = 40 P(MeOx). E) Representative ^{1}H-NMR of **6** at n = 40 P(MeOx). F) Representative MALDI of **6** at n = 40 P(MeOx). G) Possible mechanism for the observed proton-initiation.

nosylate **5** initiated polymer. Next, polymerization rates (k_p) of the three initiators were measured to compare both within, and against other previously reported initiators. A semi-logarithmic conversion plot of monomer consumption shows linear trends (R^2 = 0.9868-0.9961) with all three initiators, indicating living polymerization character (**Figure 2C**). The three initiators (**3-5**) showed agreement with literature trends in the relative magnitudes of their polymerization rates, where nosylate **5** was the fastest (6.6 x10^{-3} L mol^{-1} s^{-1}).[41] This k_p is close to a reported protected sugar containing a triflate leaving group (12.1 x10^{-3} L mol^{-1} s^{-1}) under similar conditions.[45] While mesylate initiators have not been well characterized in the P(Ox) literature, we observed that tosylate **4** and mesylate **3** have comparable rates (1.9 x10^{-3} L mol^{-1} s^{-1} and 2.8 x10^{-3} L mol^{-1} s^{-1}, respectively). Taking into consideration initiator solubility, stability, kinetics, and polymer M_n, we moved forward with nosylate **5** as the preferred initiator for the preparation of biotin-P(MeOx).

To further characterize the reactivity of initiator **5** in P(MeOx) polymerizations, the monomer:initator ([M]:[I]) feed ratio was varied. Using a microwave reactor at 140 °C, 20:1, 40:1, and 60:1 [M]:[I] all yielded polymers with low dispersities (**Figure 2B**, entries 4-6). All three P(MeOx) polymers exhibited a small amount of chain-chain coupled byproduct, as evident by the doubled molecular weight (MW) shoulder in the SEC trace (**Figure 2D**). We established k_p for MeOx at different feed ratios, as well as EtOx and NonOx using **5** at a 40:1 feed ratio at 140 °C under conventional heating conditions. The respective k_p values of the different monomers show agreement with literature trends, where MeOx polymerized the fastest, followed by EtOx, then NonOx. While relatively slow compared to other reported initiators, these rates using **5** are still practical and the polymerization can be completed in 30 minutes.

Quantification of biotin incorporation.

During our initial evaluation of initiators **3–5,** we observed biotinylation of the polymers and expected k_p trends for the initiator series. However, the discrepancy between M_n in the SEC and NMR required further investigation. We looked at biotin-P(MeOx)$_{40}$ (**6**, n = 40) as a representative example and further characterized it by NMR and matrix assisted laser desorption-time of flight (MALDI-TOF). Although the biotin peaks are prominent in the ^{1}H-NMR spectrum, the M_n of the polymer is overestimated when calculating with biotin as the end-group (**Figure 2E**). This could occur if biotin installation is not quantitative. In the MALDI spectrum, the desired biotinylated P(MeOx) was observed as the major product, though proton-initiated P(MeOx) was also observed (**Figure 2F**). This side product is well-known and characterized in the P(Ox) literature.[46,47] While relative population intensities cannot be quantified using MALDI, the amount of proton-initiated P(MeOx) seemed to be significant. Since these byproducts do not contain biotin, we sought to minimize their formation.

To estimate the percent of P(MeOx) bearing biotin, we employed a combination of NMR and SEC. By attributing overestimations in the NMR M_n solely to proton initiation, we can compare the ratio of M_n obtained by NMR to M_n obtained by SEC as an estimate. The M_n of polymers with minimal proton initiation should have excellent agreement between SEC and NMR. A screen was carried out to elucidate the condition that gives the greatest conversion for biotin initiation. A 40:1 [M]:[I] was chosen to ensure reliably high biotin signal in the NMR spectrum at an intermediate polymer size. Three solvents (DMAc, MeCN, and Sulfolane) were compared at varying concentrations (1.25 M, 2 M, 4 M) and at different temperatures (100 °C and 140 °C). Conditions at 100 °C were performed conventionally, whereas conditions at 140 °C were performed in a μwave reactor. When each condition in triplicate was compared, no statistically significant difference in biotin yield was found. We then evaluated biotin yields of synthesized poly(2-ethyl-2-oxazoline) (P(EtOx)), where proton initiation through α-proton extraction by excess monomer is suppressed due to increased steric hinderance. P(EtOx) yielded comparable amounts of proton initiation to P(MeOx) despite suppression of one possible pathway. When this experiment was attempted with poly(2-phenyl-2-oxazoline), proton-initiated polymer was also observed, despite the complete absence of an abstractable α-proton. Therefore, it is likely that the formation of proton-initiated

species is being facilitated by the biotin initiator itself, with a possible mechanism depicted in **Figure 2G**. From this condition screen, we proceeded with the DMAc, 1.25 M, 140 °C, as these gave the lowest standard deviation between yields and fast turnaround for reactions. Under these conditions, we can synthesize biotin-P(MeOx) containing between 62-70% biotin. While this percent biotinylation is comparable to previous reports quantified in the literature, this method installs biotin in a fraction of the time and does not preclude the installation of clickable handles at other positions.

Functional biotinylated P(MeOx).

Commercial biotinylated PEG is available with a plethora of different functional groups to fit various application-based needs. This functional group diversity is accessed through a core of easily transformed functional groups such as alcohols and amines. We sought to emulate this functional group versatility by synthesizing a panel of functional biotin-P(MeOx)s that can readily undergo post-polymerization modifications to yield more advanced functionality (**Scheme 2A**). We focused only on high yielding (+80%) end caps. We found that the most reliable termination occurred with polymers treated with nucleophilic salts (**6-8**) or strong nucleophiles such as thiol or hydrazine groups (**9, 10**). To demonstrate scalability, polymer **8** was synthesized and isolated at gram scale. While additional end caps utilizing carboxylic acids and amines as nucleophiles were attempted, conditions reported in the literature led to suboptimal conversion. Amines were instead accessed through the Staudinger reduction of polymer **8** using literature conditions[48] to yield biotin-P(MeOx)$_{40}$-NH$_2$ (**11**). To demonstrate the installation of advanced functionality, polymer **11** was clicked with fluorescein isothiocyanate isomer 1 to yield a hydrolytically stable fluorophore - biotinylated polymer conjugate (**12**) using previously reported conditions[49] (**Scheme 2B**)

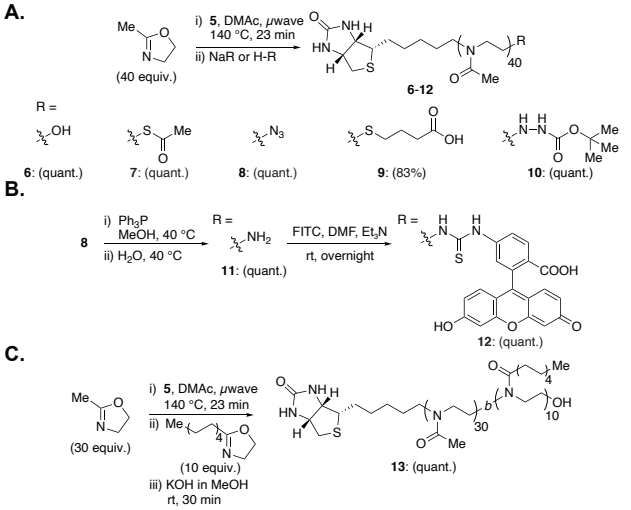

Scheme 2. End group panel of biotin-P(MeOx). A) Terminal functionalization with strong nucleophiles. B) Post polymerization modification of biotin-P(MeOx). C) Synthesis of biotinylated diblock co-polymer P(Ox) surfactant.

A key feature of living polymerizations is the ease of synthesis of block copolymers. By using biotinylated initiators, biotin functionalized diblock co-polymers can be readily accessed with distinct sizes and block identities. Biotinylated micelles and nanoemulsions can then be assembled for *in vivo* applications using these surfactants. Currently, the only commercially available biotin-PEG surfactant is 1,2-distearoyl-sn-glycero-3-phosphoethanolamine-*N*-[biotinyl(polyethylene glycol)] which, while useful, is not sufficient when flexibility in polymer size and block ratio is needed. To showcase biotin amphiphile preparation, biotin-P(MeOx)$_{30}$-*b*-P(NonOx)$_{10}$ surfactant (**13**) was synthesized. These block lengths were chosen as our lab has previously employed similar surfactants to stabilize perfluorocarbon-in-water nanoemulsions, though a wide range of oxazoline monomers or block ratios can be achieved following established P(Ox) literature (**Scheme 2C**).[50]

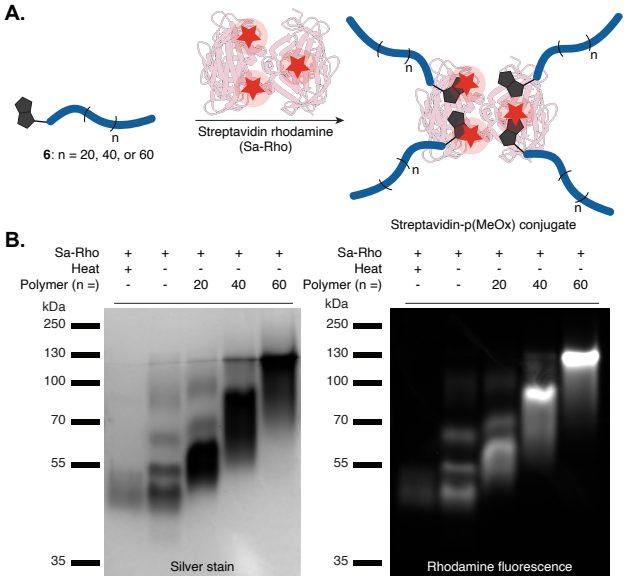

Figure 3. Gel shift assay of streptavidin. A) Schematic of the gel shift assay. B) 12% SDS-PAGE gel showing size dependent shift of streptavidin with silver (left) and unstained fluorescence (right). Heated samples were mixed with Laemmli sample buffer, then boiled at 100 °C for 2 hours. Unheated samples were mixed with Laemmli buffer immediately prior to running.

Binding to streptavidin.

With the ability to synthesize biotin-P(MeOx) of different lengths and terminal end functional groups, we sought to validate that these polymers bind to streptavidin, and that neither the reduction of the biotin nor the roughly 30% proton-initiated P(MeOx) present debilitates their performance. We evaluated binding performance through a gel shift assay, a fluorescence resonance energy transfer (FRET) experiment, and through nanoparticle labelling – three popular applications of biotinylated hydrophilic polymers.

Beginning with the gel shift assay, we synthesized polymer **6** at three different degrees of polymerization: n = 20, 40, and 60. Since streptavidin is a tetrameric protein capable of binding to biotin at four different sites, we expected

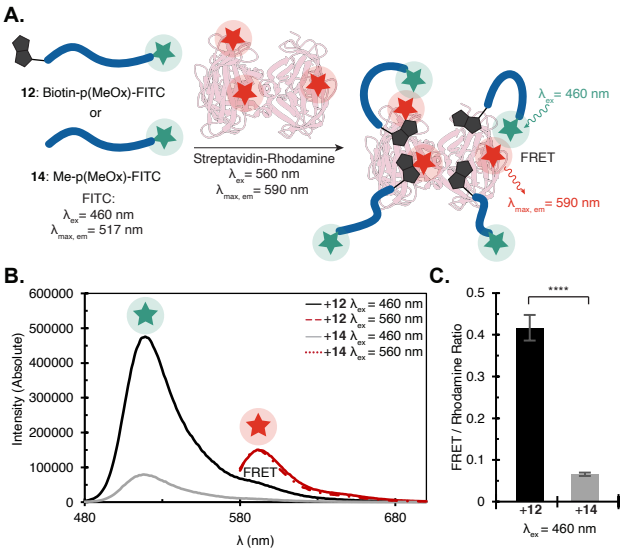

Figure 4. FRET utilizing biotin-P(MeOx)-FITC and Sa-Rho. A) Schematic of FRET experiment. Sa-Rho was incubated with 12.5 equivalents of either **13** or **14** for 30 minutes, then dialyzed (10,000 MWCO). The proteins were then washed six times using 10,000 MWCO spin filters. B) Fluorescence traces of **12** and **14** treated Sa-Rho. C) Quantification of the FRET / rhodamine emission ratio. Emission: 460 nm, slit width excitation 1 nm, slit width emission 1 nm.

the protein to gain molecular weight correlating to the size of the polymer bound (**Figure 3A**). Sodium dodecyl sulfate polyacrylamide gel electrophoresis (SDS-PAGE) was employed to visualize the shift in mass. The three polymers (**6**) each were incubated with commercial streptavidin-rhodamine (Sa-Rho). As a negative control, two samples of Sa-Rho were incubated with **1**, with or without boiling. The samples containing polymer were not boiled. The five samples were run, imaged for rhodamine fluorescence, and then visualized with silver stain. Sa-Rho that was not boiled showed higher amounts of aggregation above the tetramer, though higher order aggregates above 70 kDa were not abundant. Sa-Rho treated with polymers showed a noticeable increase in the size of the protein and this difference became more drastic as the molecular weight of the polymer increased, indicating successful binding (**Figure 3B**).

Next, we conducted a FRET experiment using Sa-Rho and FITC-conjugated **12** to demonstrate binding between biotin-initiated **12** and streptavidin. We synthesized the previously reported Me-P(MeOx)-FITC (**14**) as a negative control.[49] We coincubated 12.5 equivalents (per binding site) of **12** (or **14**) with Sa-Rho for 30 minutes, dialyzed (10,000 MWCO), then centrifuged the samples over a spin filter (10,000 Da MWCO) to remove excess polymer (**Figure 4A**). After ensuring that similar amounts of Sa-Rho were present via excitation at 560 nm (**Figure 4B**, red), the samples were excited at 460 nm and the total fluorescence and rhodamine fluorescence were analyzed (**Figure 4B,** black, grey). Comparing the emission upon 460 nm excitation clearly demonstrates that biotin is necessary to retain significant fluorescence and FRET signal. The minimal amount of persistent fluorescence from nonbiotinylated polymer **14** is likely due to nonspecific binding to Sa-Rho. Quantification of these data using the total rhodamine signal (excited at 560 nm) as normalization shows a 6.4-fold increase in the FRET signal observed for **12**-treated Sa-Rho over **14**-treated Sa-Rho (**Figure 4C**). These results further support that biotin-initiated P(MeOx) shows strong binding to streptavidin.

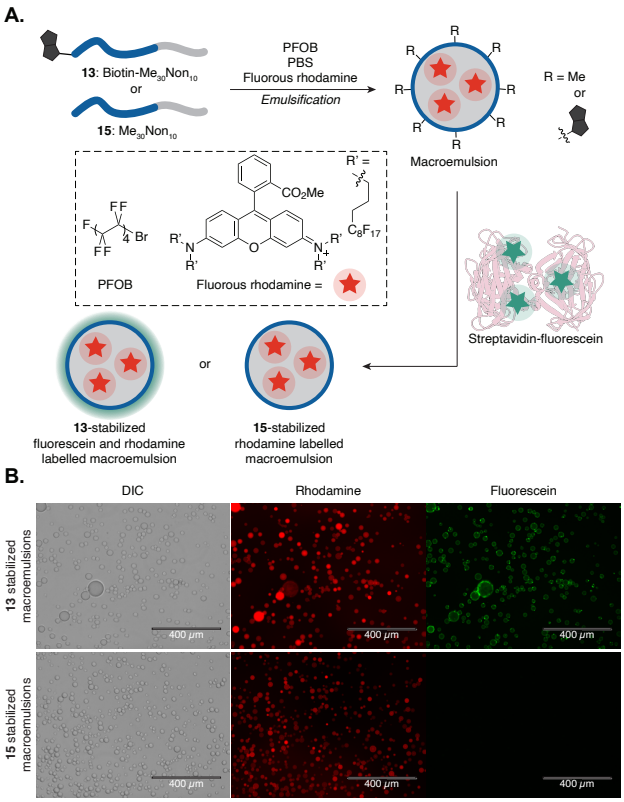

Figure 5. Streptavidin labelled macroemulsions. A) Formulation of biotinylated and nonbiotinylated macroemulsions. Emulsions were incubated with 0.5 mg/mL Sa-Fluo for 20 minutes. The supernatant was replaced three times with phosphate buffered saline (PBS) to remove excess protein. Emulsions were diluted 1 in 20 in PBS for imaging at 10x magnification. B) Microscopy images of **13** stabilized macroemulsions treated as described in (A). Differential interference contrast (DIC), red channel, green channel (left to right). Microscopy images of **15** stabilized macroemulsions. DIC, red channel, green channel (left to right). Scale bars represent 400 μm.

Finally, we demonstrated that biotin-P(Ox) amphiphiles can be used to make biotinylated nanoparticles which subsequently associate with streptavidin. Biotinylated block copolymer **13** was used to make perfluorocarbon-in-water macroemulsions. These emulsions were compared to those prepared from previously reported Me-P(MeOx)$_{30}$-P(NonOx)$_{10}$ (**15**).[51] Macroemulsions were prepared by mixing a 1:6.6 ratio of perfluorooctyl bromide containing 50 nM fluorous soluble rhodamine to PBS with 0.2 mM surfactant and shaking (**Figure 5A**).[52] The macroemulsion solutions were there subjected to 100 uL of 1 mg/mL streptavidin-fluorescein (Sa-Fluo)[53] and imaged via epifluorescence microscopy. Samples containing **13** showed clear labelling with both the fluorous rhodamine inside the emulsion and the Sa-Fluo adhered to the surface (**Figure 5B**). Comparatively, surfactant **15** stabilized emulsions displayed rhodamine fluorescence yet did not exhibit Sa-Fluo labelling, indicating that the biotin is necessary for the interaction and that nonspecific labelling is minimal.

Conclusions.

We have demonstrated that biotin can be directly installed onto P(Ox) scaffolds through initiation. Biotinol was transformed into a nosylate (**5**), which demonstrated living polymerization character and a modest k_p at 140 °C for 2-methyl-2-oxazoline polymerization. Biotin-P(MeOx) was synthesized in a variety of molecular weights with up to 70% biotin incorporation, with the remaining percentage characterized as proton-initiated P(MeOx). Standard termination reagents can be used to produce bifunctional P(MeOx) polymers. The biotin-initiation strategy is compatible with post-polymerization modification as demonstrated by the installation of fluorescein on P(MeOx). Initiation of other oxazoline monomers and the formation of block copolymers was also successful with nosylate **5.**

The ability for biotin-P(MeOx) to bind streptavidin was evaluated through three assays. Gel shift assays showed an M_n-dependent increase in molecular weight when streptavidin was bound to several different sized biotin-P(MeOx)s. Biotin-P(MeOx)-FITC was retained through extensive purification when bound to streptavidin. This pair showed enhanced fluorescein and FRET signals compared to streptavidin treated with the non-biotinylated control. Lastly, perfluorocarbon macroemulsions displaying biotin on the surface were formulated. Selective labelling of these macroemulsions using streptavidin-fluorescein over non-biotinylated macroemulsions was shown. These assays demonstrate the viability of biotin-initiated P(Ox) for use in applications commonly used with biotin polymers. Overall, this route to installing biotin retains the capacity for post-polymerization click chemistry and offers significant promise in developing highly functionalized PEG replacements.

AUTHOR INFORMATION

Corresponding Author

Ellen M. Sletten – *Department of Chemistry and Biochemistry, University of California, Los Angeles, Los Angeles, California 90095, United States;* orcid.org/0000-0002-0049-7278; Email: sletten@chem.ucla.edu

Authors

Joseph A. Garcia – *Department of Chemistry and Biochemistry, University of California, Los Angeles, Los Angeles, California 90095, United States;* orcid.org/ 0000-0002-0253-3121

Ashley Vergara Mendez – *Department of Chemistry and Biochemistry, University of California, Los Angeles, Los Angeles, California 90095, United States;* orcid.org/0009-0002-9459-9829

Notes

The authors declare no competing financial interest.

ACKNOWLEDGMENT

Funding was provided by the following grants: Eugine V. Cota Robles to J.A.G., National Institute of General Medical Sciences of the National Institutes of Health (R01GM135380) to E.M.S. NMR data were obtained on instruments funded by the National Science Foundation (MRICHE-1048804). The authors thank the Backus group for equipment, and to Eli Biletch for training on the ChemiDoc Imaging System. They thank Helen Lin for the synthesis of fluorous rhodamine.

REFERENCES

(1) Green, N. M. Avidin. In *Advances in Protein Chemistry*; Anfinsen, C. B., Edsall, J. T., Richards, F. M. B. T.-A. in P. C., Eds.; Academic Press, 1975; Vol. 29, pp 85–133. DOI: 10.1016/S0065-3233(08)60411-8.

(2) McConnell, D. B. Biotin's Lessons in Drug Design. *J. Med. Chem.* **2021**, *64* (22), 16319–16327. DOI: 10.1021/acs.jmedchem.1c00975.

(3) Ishii, Y.; Kondo, K.; Matsumoto, T.; Tanaka, K.; Shinkai-Ouchi, F.; Hagiwara, K.; Kanda, T. Thiol-Reactive Reagents Inhibits Intracellular Trafficking of Human Papillomavirus Type 16 Pseudovirions by Binding to Cysteine Residues of Major Capsid Protein L1. *Virol. J.* **2007**, *4* (1), 110. DOI: 10.1186/1743-422X-4-110.

(4) Laner-Plamberger, S.; Oeller, M.; Poupardin, R.; Krisch, L.; Hochmann, S.; Kalathur, R.; Pachler, K.; Kreutzer, C.; Erdmann, G.; Rohde, E.; Strunk, D.; Schallmoser, K. Heparin Differentially Impacts Gene Expression of Stromal Cells from Various Tissues. *Sci. Rep.* **2019**, *9* (1), 7258. DOI: 10.1038/s41598-019-43700-x.

(5) Strachan, E.; Mallia, A. K.; Cox, J. M.; Antharavally, B.; Desai, S.; Sykaluk, L.; O'Sullivan, V.; Bell, P. A. Solid-Phase Biotinylation of Antibodies. *J. Mol. Recognit.* **2004**, *17* (3), 268–276. DOI: 10.1002/jmr.669.

(6) Kuzmin, A.; Poloukhtine, A.; Wolfert, M. A.; Popik, V. V. Surface Functionalization Using Catalyst-Free Azide-Alkyne Cycloaddition. *Bioconjug. Chem.* **2010**, *21* (11), 2076–2085. DOI: 10.1021/bc100306u.

(7) Degirmenci, A.; Yeter Bas, G.; Sanyal, R.; Sanyal, A. "clickable" Polymer Brush Interfaces: Tailoring Monovalent to Multivalent Ligand Display for Protein Immobilization and Sensing. *Bioconjug. Chem.* **2022**, *33* (9), 1672–1684. DOI: 10.1021/acs.bioconjchem.2c00298.

(8) Sun, X. L.; Faucher, K. M.; Houston, M.; Grande, D.; Chaikof, E. L. Design and Synthesis of Biotin Chain-Terminated Glycopolymers for Surface Glycoengineering. *J. Am. Chem. Soc.* **2002**, *124* (25), 7258–7259. DOI: 10.1021/ja025788v.

(9) Xue, Y.; Li, J.; Yang, G.; Liu, Z.; Zhou, H.; Zhang, W. Multistep Consolidated Phototherapy Mediated by a NIR-Activated Photosensitizer. *ACS Appl. Mater. Interfaces* **2019**, *11* (37), 33628–33636. DOI: 10.1021/acsami.9b10605.

(10) Ouchi, T.; Yamabe, E.; Hara, K.; Hirai, M.; Ohya, Y. Design of Attachment Type of Drug Delivery System by Complex Formation of Avidin with Biotinyl Drug Model and Biotinyl Saccharide. *J. Control. Release* **2004**, *94* (2), 281–291. DOI: https://doi.org/10.1016/j.jconrel.2003.09.020.

(11) Chen, Y.; Meng, W.; Chen, M.; Zhang, L.; Chen, M.; Chen, X.; Peng, J.; Huang, N.; Zhang, W.; Chen, J. Biotin-Decorated Hollow Gold Nanoshells for Dual-Modal Imaging-Guided NIR-II Photothermal and Radiosensitizing Therapy toward Breast Cancer. *J. Mater. Chem. B* **2023**, *11* (41), 10003–10018. DOI: 10.1039/D3TB01736B.

(12) Wang, Y.; van Steenbergen, M. J.; Beztsinna, N.; Shi, Y.; Lammers, T.; van Nostrum, C. F.; Hennink, W. E. Biotin-Decorated All-HPMA Polymeric Micelles for Paclitaxel Delivery. *J. Control. Release* **2020**, *328*, 970–984. DOI: https://doi.org/10.1016/j.jconrel.2020.09.013.

(13) Cheng, C.; Wei, H.; Zhu, J. L.; Chang, C.; Cheng, H.; Li, C.; Cheng, S. X.; Zhang, X. Z.; Zhuo, R. X. Functionalized Thermoresponsive Micelles Self-Assembled from Biotin-PEG-b-P(NIPAAm-Co-HMAAm)-b-PMMA for Tumor Cell Target. *Bioconjug. Chem.* **2008**, *19* (6), 1194–1201. DOI: 10.1021/bc8000062.

(14) Mok, H.; Ji, W. P.; Tae, G. P. Enhanced Intracellular Delivery of Quantum Dot and Adenovirus Nanoparticles Triggered by Acidic PH via Surface Charge Reversal. *Bioconjug. Chem.* **2008**, *19* (4), 797–801. DOI: 10.1021/bc700464m.

(15) Traina, C. A.; Bakus, R. C.; Bazan, G. C. Design and Synthesis of Monofunctionalized, Water-Soluble Conjugated Polymers for Biosensing and Imaging Applications. *J. Am.*

Chem. Soc. **2011**, *133* (32), 12600–12607. DOI: 10.1021/ja202877q.

(16) Zheng, J.; Swager, T. M. Biotinylated Poly(p-Phenylene Ethynylene): Unexpected Energy Transfer Results in the Detection of Biological Analytes. *Chem. Commun.* **2004**, No. 24, 2798–2799. DOI: 10.1039/b408478k.

(17) VanVeller, B.; Swager, T. M. Biocompatible Post-Polymerization Functionalization of a Water Soluble Poly(p-Phenylene Ethynylene). *Chem. Commun.* **2010**, *46* (31), 5761–5763. DOI: 10.1039/c0cc01456g.

(18) Harker, E. A.; Daniels, D. S.; Guarracino, D. A.; Schepartz, A. β-Peptides with Improved Affinity for HDM2 and HDMX. *Bioorganic Med. Chem.* **2009**, *17* (5), 2038–2046. DOI: 10.1016/j.bmc.2009.01.039.

(19) Schumann, B.; Malaker, S. A.; Wisnovsky, S. P.; Debets, M. F.; Agbay, A. J.; Fernandez, D.; Wagner, L. J. S.; Lin, L.; Li, Z.; Choi, J.; Fox, D. M.; Peh, J.; Gray, M. A.; Pedram, K.; Kohler, J. J.; Mrksich, M.; Bertozzi, C. R. Bump-and-Hole Engineering Identifies Specific Substrates of Glycosyltransferases in Living Cells. *Mol. Cell* **2020**, *78* (5), 824-834.e15. DOI: https://doi.org/10.1016/j.molcel.2020.03.030.

(20) Lyu, Z.; Zhao, Y.; Buuh, Z. Y.; Gorman, N.; Goldman, A. R.; Islam, M. S.; Tang, H.-Y.; Wang, R. E. Steric-Free Bioorthogonal Labeling of Acetylation Substrates Based on a Fluorine–Thiol Displacement Reaction. *J. Am. Chem. Soc.* **2021**, *143* (3), 1341–1347. DOI: 10.1021/jacs.0c05605.

(21) Hashimoto, K.; Loader, J. E.; Kinsky, S. C. Iodoacetylated and Biotinylated Liposomes: Effect of Spacer Length on Sulfhydryl Ligand Binding and Avidin Precipitability. *Biochim. Biophys. Acta - Biomembr.* **1986**, *856* (3), 556–565. DOI: https://doi.org/10.1016/0005-2736(86)90147-1.

(22) Lacorn, M.; Fleischer, K.; Willig, S.; Gremmel, S.; Steinhart, H.; Claus, R. Use of Biotinylated 17β-Estradiol in Enzyme-Immunoassay Development: Spacer Length and Chemical Structure of the Bridge Are the Main Determinants in Simultaneous Streptavidin-Antibody Binding. *J. Immunol. Methods* **2005**, *297* (1–2), 225–236. DOI: 10.1016/j.jim.2004.12.011.

(23) D'souza, A. A.; Shegokar, R. Polyethylene Glycol (PEG): A Versatile Polymer for Pharmaceutical Applications. *Expert Opin. Drug Deliv.* **2016**, *13* (9), 1257–1275. DOI: 10.1080/17425247.2016.1182485.

(24) Knop, K.; Hoogenboom, R.; Fischer, D.; Schubert, U. S. Poly(Ethylene Glycol) in Drug Delivery: Pros and Cons as Well as Potential Alternatives. *Angew. Chemie - Int. Ed.* **2010**, *49* (36), 6288–6308. DOI: 10.1002/anie.200902672.

(25) Yang, Q.; Jacobs, T. M.; McCallen, J. D.; Moore, D. T.; Huckaby, J. T.; Edelstein, J. N.; Lai, S. K. Analysis of Pre-Existing IgG and IgM Antibodies against Polyethylene Glycol (PEG) in the General Population. *Anal. Chem.* **2016**, *88* (23), 11804–11812. DOI: 10.1021/acs.analchem.6b03437.

(26) Vázquez-Dorbatt, V.; Maynard, H. D. Biotinylated Glycopolymers Synthesized by Atom Transfer Radical Polymerization. *Biomacromolecules* **2006**, *7* (8), 2297–2302. DOI: 10.1021/bm060105f.

(27) Bontempo, D.; Li, R. C.; Ly, T.; Brubaker, C. E.; Maynard, H. D. One-Step Synthesis of Low Polydispersity, Biotinylated Poly(N-Isopropylacrylamide) by ATRP. *Chem. Commun.* **2005**, No. 37, 4702–4704. DOI: 10.1039/B507912H.

(28) Hou, S.; Sun, X.-L.; Dong, C.-M.; Chaikof, E. L. Facile Synthesis of Chain-End Functionalized Glycopolymers for Site-Specific Bioconjugation. *Bioconjug. Chem.* **2004**, *15* (5), 954–959. DOI: 10.1021/bc0499275.

(29) Qi, K.; Ma, Q.; Remsen, E. E.; Clark, C. G.; Wooley, K. L. Determination of the Bioavailability of Biotin Conjugated onto Shell Cross-Linked (SCK) Nanoparticles. *J. Am. Chem. Soc.* **2004**, *126* (21), 6599–6607. DOI: 10.1021/ja039647k.

(30) Hong, C.-Y.; Pan, C.-Y. Direct Synthesis of Biotinylated Stimuli-Responsive Polymer and Diblock Copolymer by RAFT Polymerization Using Biotinylated Trithiocarbonate as RAFT Agent. *Macromolecules* **2006**, *39* (10), 3517–3524. DOI: 10.1021/ma052593+.

(31) Viegas, T. X.; Bentley, M. D.; Harris, J. M.; Fang, Z.; Yoon, K.; Dizman, B.; Weimer, R.; Mero, A.; Pasut, G.; Veronese, F. M. Polyoxazoline: Chemistry, Properties, and Applications in Drug Delivery. *Bioconjug. Chem.* **2011**, *22* (5), 976–986. DOI: 10.1021/bc200049d.

(32) Hoogenboom, R. Poly(2-Oxazoline)s: A Polymer Class with Numerous Potential Applications. *Angew. Chemie - Int. Ed.* **2009**, *48* (43), 7978–7994. DOI: 10.1002/anie.200901607.

(33) Moreadith, R. W.; Viegas, T. X.; Bentley, M. D.; Harris, J. M.; Fang, Z.; Yoon, K.; Dizman, B.; Weimer, R.; Rae, B. P.; Li, X.; Rader, C.; Standaert, D.; Olanow, W. Clinical Development of a Poly(2-Oxazoline) (POZ) Polymer Therapeutic for the Treatment of Parkinson's Disease – Proof of Concept of POZ as a Versatile Polymer Platform for Drug Development in Multiple Therapeutic Indications. *Eur. Polym. J.* **2017**, *88*, 524–552. DOI: œ.

(34) Pretzer, I.; Bushiri, D.; Weberskirch, R. Biotin-Functionalized Block Catiomers as an Active Targeting Approach in Gene Delivery. *Macromol. Mater. Eng.* **2023**, *308* (6), 2200627. DOI: 10.1002/mame.202200627.

(35) Brož, P.; Benito, S. M.; Saw, C.; Burger, P.; Heider, H.; Pfisterer, M.; Marsch, S.; Meier, W.; Hunziker, P. Cell Targeting by a Generic Receptor-Targeted Polymer Nanocontainer Platform. *J. Control. Release* **2005**, *102* (2), 475–488. DOI: https://doi.org/10.1016/j.jconrel.2004.10.014.

(36) Verbraeken, B.; Monnery, B. D.; Lava, K.; Hoogenboom, R. The Chemistry of Poly(2-Oxazoline)S. *Eur. Polym. J.* **2017**, *88*, 451–469. DOI: 10.1016/j.eurpolymj.2016.11.016.

(37) Wright, L. D.; Skeggs, H. R.; Cresson, E. L. Amides and Amino Acid Derivatives of Biotin: Microbiological Studies. *J. Am. Chem. Soc.* **1951**, *73* (9), 4144–4145. DOI: 10.1021/ja01153a028.

(38) Paulus, R. M.; Becer, C. R.; Hoogenboom, R.; Schubert, U. S. Acetyl Halide Initiator Screening for the Cationic Ring-Opening Polymerization of 2-Ethyl-2-Oxazoline. *Macromol. Chem. Phys.* **2008**, *209* (8), 794–800. DOI: https://doi.org/10.1002/macp.200700506.

(39) Weber, C.; Becer, R. C.; Baumgaertel, A.; Hoogenboom, R.; Schubert, U. S. Preparation of Methacrylate End-Functionalized Poly(2-Ethyl-2-Oxazoline) Macromonomers. *Des. Monomers Polym.* **2009**, *12* (2), 149–165. DOI: 10.1163/156855509X412090.

(40) Hoogenboom, R.; Fijten, M. W. M.; Schubert, U. S. Parallel Kinetic Investigation of 2-Oxazoline Polymerizations with Different Initiators as Basis for Designed Copolymer Synthesis. *J. Polym. Sci. Part A Polym. Chem.* **2004**, *42* (8), 1830–1840. DOI: https://doi.org/10.1002/pola.20024.

(41) Glassner, M.; D'Hooge, D. R.; Young Park, J.; Van Steenberge, P. H. M.; Monnery, B. D.; Reyniers, M. F.; Hoogenboom, R. Systematic Investigation of Alkyl Sulfonate Initiators for the Cationic Ring-Opening Polymerization of 2-Oxazolines Revealing Optimal Combinations of Monomers and Initiators. *Eur. Polym. J.* **2015**, *65*, 298–304. DOI: 10.1016/j.eurpolymj.2015.01.019.

(42) Damont, A.; Boisgard, R.; Dollé, F.; Hollocou, M.; Kuhnast, B. Avidin/Biotin Bioinspired Platform for Dual In Vivo 18F-PET/NIRF Molecular Imaging. *Bioconjug. Chem.* **2017**, *28* (10), 2524–2529. DOI: 10.1021/acs.bioconjchem.7b00536.

(43) Islam, I.; Ng, K. yun; Chong, K. T.; McQuade, T. J.; Hui, J. O.; Wilkinson, K. F.; Rush, B. D.; Ruwart, M. J.; Borchardt, R. T.; Fisher, J. F. Evaluation of a Vitamin-Cloaking Strategy for Oligopeptide Therapeutics: Biotinylated HIV-1 Protease Inhibitors. *J. Med. Chem.* **1994**, *37* (2), 293–304. DOI: 10.1021/jm00028a013.

(44) Hoogenboom, R.; Paulus, R. M.; Fijten, M. W. M.; Schubert, U. S. Concentration Effects in the Cationic Ring-Opening Polymerization of 2-Ethyl-2-Oxazoline in N,N-Dimethylacetamide. *J. Polym. Sci. Part A Polym. Chem.* **2005**, *43* (7), 1487–1497. DOI: https://doi.org/10.1002/pola.20603.

(45) Weber, C.; Czaplewska, J. A.; Baumgaertel, A.; Altuntas, E.; Gottschaldt, M.; Hoogenboom, R.; Schubert, U. S. A Sugar Decorated Macromolecular Bottle Brush by Carbohydrate-Initiated Cationic Ring-Opening Polymerization. *Macromolecules* **2012**, *45* (1), 46–55. DOI:

10.1021/ma202401x.
(46) Brunzel, M.; Dirauf, M.; Sahn, M.; Czaplewska, J. A.; Fritz, N.; Weber, C.; Nischang, I.; Schubert, U. S. On the Identification and Quantification of Proton-Initiated Species in the Synthesis of Poly(2-Alkyl-2-Oxazoline)s by High Resolution Liquid Chromatography. *J. Chromatogr. A* **2021**, *1653*, 462364. DOI: https://doi.org/10.1016/j.chroma.2021.462364.
(47) Litt, M.; Levy, A.; Herz, J. Polymerization of Cyclic Imino Ethers. X. Kinetics, Chain Transfer, and Repolymerization. *J. Macromol. Sci. Part A - Chem.* **1975**, *9* (5), 703–727. DOI: 10.1080/00222337508065890.
(48) Osawa, S.; Ishii, T.; Takemoto, H.; Osada, K.; Kataoka, K. A Facile Amino-Functionalization of Poly(2-Oxazoline)s' Distal End through Sequential Azido End-Capping and Staudinger Reactions. *Eur. Polym. J.* **2017**, *88*, 553–561. DOI: https://doi.org/10.1016/j.eurpolymj.2016.11.029.
(49) Sedlacek, O.; Janouskova, O.; Verbraeken, B.; Hoogenboom, R. Straightforward Route to Superhydrophilic Poly(2-Oxazoline)s via Acylation of Well-Defined Polyethylenimine. *Biomacromolecules* **2019**, *20* (1), 222–230. DOI: 10.1021/acs.biomac.8b01366.
(50) Day, R. A.; Estabrook, D. A.; Wu, C.; Chapman, J. O.; Togle, A. J.; Sletten, E. M. Systematic Study of Perfluorocarbon Nanoemulsions Stabilized by Polymer Amphiphiles. *ACS Appl. Mater. Interfaces* **2020**, *12* (35), 38887–38898. DOI: 10.1021/acsami.0c07206.
(51) Estabrook, D. A.; Ennis, A. F.; Day, R. A.; Sletten, E. M. Controlling Nanoemulsion Surface Chemistry with Poly(2-Oxazoline) Amphiphiles. *Chem. Sci.* **2019**, *10* (14), 3994–4003. DOI: 10.1039/C8SC05735D.
(52) Sletten, E. M.; Swager, T. M. Fluorofluorophores: Fluorescent Fluorous Chemical Tools Spanning the Visible Spectrum. *J. Am. Chem. Soc.* **2014**, *136* (39), 13574–13577. DOI: 10.1021/ja507848f.
(53) Lucio, A. A.; Ingber, D. E.; Campàs, O. Chapter 20 - Generation of Biocompatible Droplets for in Vivo and in Vitro Measurement of Cell-Generated Mechanical Stresses. In *Biophysical Methods in Cell Biology*; Paluch, E. K. B. T.-M. in C. B., Ed.; Academic Press, 2015; Vol. 125, pp 373–390. DOI: https://doi.org/10.1016/bs.mcb.2014.11.008.